

TNO PUBLIC

TNO report

TNO 2020 R11609

Report on Task 4 of project "SVOW OGP JIP airgun measurements": Reporting

Defence, Safety & Security

Oude Waalsdorperweg 63 2597 AK Den Haag P.O. Box 96864 2509 JG The Hague The Netherlands

www.tno.nl

T +31 88 866 10 00

Date May 2021

Author(s) Mark Prior (TNO)

Michael Ainslie (JASCO)

Michele Halvorsen (Formerly CSA, now UNH)

Iris Hartstra (TNO)

Robert Laws(Havakustik Ltd) Alex MacGillivray (JASCO)

Roel Müller (TNO) Lian Wang (NPL) Stephen Robinson (NPL) Ad van Heijningen (TNO)

No. of copies 1 hard copy & 1 cd Number of pages 35 (incl. appendices)

Number of appendices 3

Sponsor International Association of Oil & Gas Producers (IOGP)

Project name "Airgun Signature and Sound Field Characterization using

Svein Vaage single Airgun and Airgun Cluster Measurements",

Contract JIP22 III-15-13; Schedule No.: 04 (III-17)

Project number 060.15171

All rights reserved.

No part of this publication may be reproduced and/or published by print, photoprint, microfilm or any other means without the previous written consent of TNO.

In case this report was drafted on instructions, the rights and obligations of contracting parties are subject to either the General Terms and Conditions for commissions to TNO, or the relevant agreement concluded between the contracting parties. Submitting the report for inspection to parties who have a direct interest is permitted.

© 2021 TNO

Summary

Measurements of sound emitted from airguns and airgun clusters are described. Measurements were made in 2007 and 2009-2010 in fjord environments in Norway and for various airgun types, chamber pressures, operating depths and airgun volumes. For each combination of these parameters, a sequence of up to 50 shots was performed, resulting in a few tens of thousands of shots recorded on approximately 20 hydrophone channels at a variety of positions. The measurements were made to establish a definitive dataset to characterize the acoustical properties of single airguns and airgun clusters. The data were intended for calibration and validation of airgun modelling tools, including those capable of producing estimates at angles and frequencies outside the ranges typically used for seismic imaging.

Summaries are given of the procedure whereby the dataset was pre-processed and subsequently used to characterise the acoustic output of all subject airguns. A summary is also made of the validation of the characterisations by comparison of sound pressures predicted using those characterisations and measured on far-field hydrophones during data acquisition. References are made to interim reports in which more details of these activities are available.

The format of a dataset containing the results of the processing is described.

Contents

	Summary	2
1	Introduction	4
1.1	Background	
1.2	Task 4 objective	6
2	Summary of Task 1: Characterize sound pressure measurements	7
2.1	Data availability	7
2.2	Channel recommendations	7
2.3	Pre-processing	11
2.4	Bioacoustic metrics	11
2.5	Results	12
3	Summary of Task 2: Characterize sources	13
4	Summary of Task 3: Predict sound field / far-field source signature	18
5	Data format of Numerical Project Outputs	21
6	Discussion and Recommendations	22
7	Conclusions	23
8	References	24
9	Signature	25

Appendices

- A Additions to Underwater Acoustics Terminology Arising from the Study
- B Data format of numerical project output
- C Comprehensive overview of source waveforms and spectra

1 Introduction

1.1 Background

There is increasing scientific and societal interest in the potential impact on marine life of sound generated by compressed air sources (airguns) during marine-seismic surveys. Fundamental to any objective analysis of this topic is an understanding of the properties of airguns as sound sources, both individually and when deployed in arrays.

The E&P Sound and Marine Life Joint Industry Programme (henceforth abbreviated "JIP") commissioned PGS Geophysical to conduct measurements of sound emitted from airguns and airgun clusters. Measurements were carried out in 2007 and 2009-2010 using equipment suspended from barges in Hjørunfjord and Storfjorden, Norway. This dataset is referred to henceforth as the "Svein Vaage data" and is suitable for use to characterize the acoustical properties of individual airguns and airgun clusters.

For each airgun type, measurements were made for a number of different combinations of chamber pressure, operating depth and airgun volume. For each combination, a sequence of up to 50 shots was performed, resulting in a few tens of thousands of shots recorded on approximately 20 hydrophone channels at a variety of positions. These recordings had a sampling rate up to 102.4 kHz (Nyquist up to 51.2 kHz), resulting in approximately half a million shot-channel combinations and 660 gigabytes of data.

The Svein Vaage data were gathered to establish a definitive dataset to characterize the acoustical properties of single airguns and airgun clusters. The data were intended for calibration and validation of airgun modelling tools, including those capable of producing estimates at angles and frequencies beyond the range typically used for seismic imaging. The original Svein Vaage data exist in SEG-Y format along with documentation and initial QA/QC information.

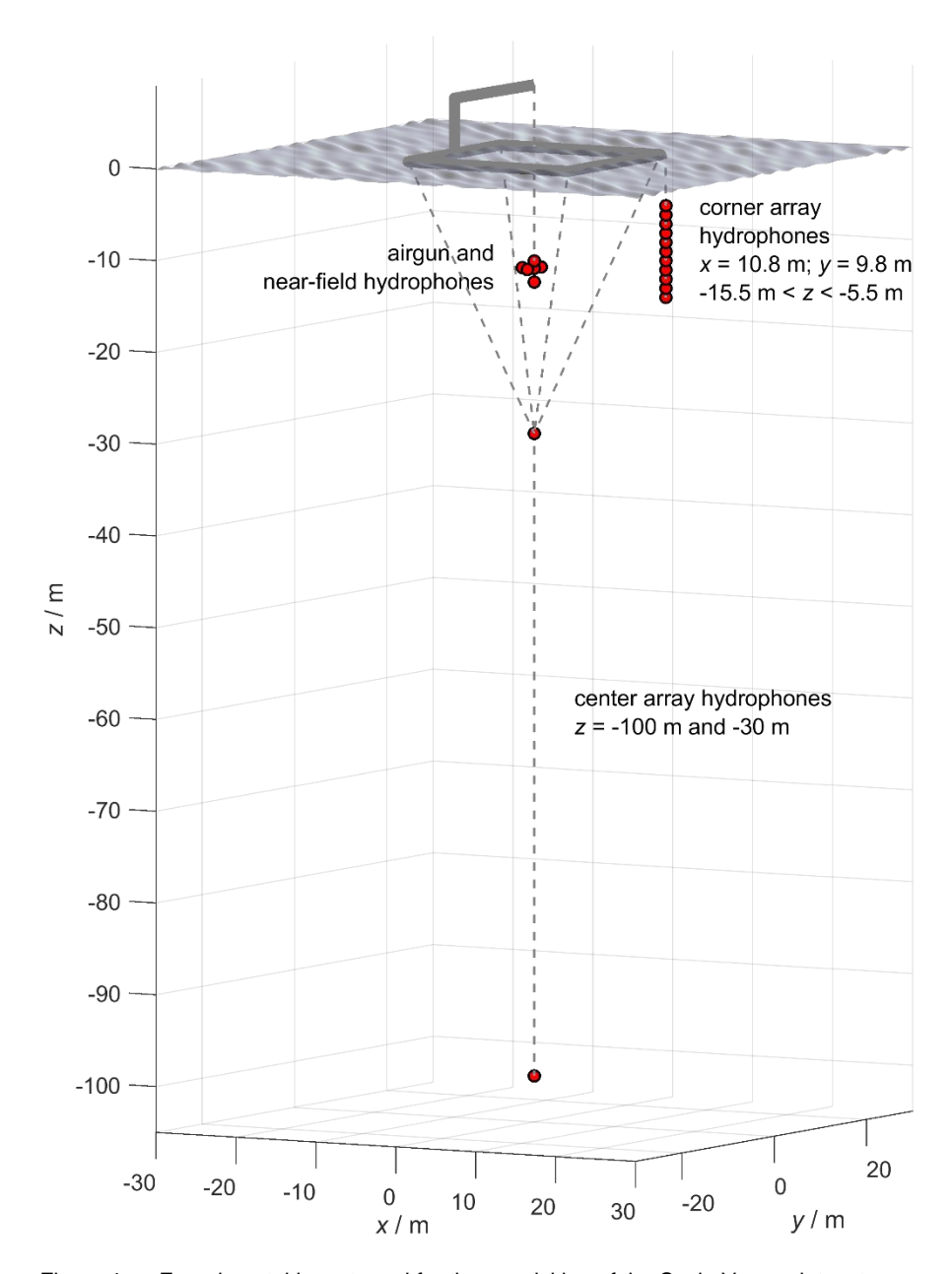


Figure 1 Experimental layout used for the acquisition of the Svein Vaage dataset.

One potential use of the Svein Vaage data is to provide ground truth for the purpose of validating or calibrating source models such as Gundalf, AASM, Agora and Nucleus, including at high frequencies. In order to achieve this, it is first necessary to convert the measurements of the received sound pressure field into a property of the source, such as its time-domain waveform or its frequency-domain spectrum.

In July 2016, an international workshop was held in Dublin [Ainslie et al., 2016] to identify and understand differences in predictions of source signature and sound propagation for well specified scenarios. Its main findings were:

- Relatively small (1-5 dB) differences were found between model predictions of low frequency signatures (frequencies up to 200 Hz, primarily of interest for imaging).
- Large (up to 35 dB) differences were found between model predictions of high frequency signatures (frequencies above 1 kHz, primarily of interest for environmental impact assessment). There is a need for measurements before further progress can be made with resolving the observed differences in the predictions of the high frequency sound field.

The Svein Vaage dataset provides a valuable opportunity to build on the Dublin workshop by providing the measurements with which to build confidence in the high frequency signature models.

In December 2016, TNO submitted a proposal [TNO, 2016] to the JIP describing the scope of a proposed review of the Svein Vaage data and addressing comments and requests received from the JIP after the submission of a pre-proposal. The proposal was accepted and a project begun in September 2017. The project was divided into a series of tasks, the fourth of which is the subject of this report.

1.2 Task 4 objective

This report provides a summary of the work carried out in first three tasks within the project [TNO, 2016]:

- Task 1: Characterize sound pressure measurements
- Task 2: Characterize sources
- Task 3: Predict sound field / far-field source signature.

The report is intended to provide a synopsis of the dataset and an executive summary of the work carried out to produce it. A description is also provided of the format of the files in which the project output is stored.

The acoustical terminology used in this report follows ISO 18405 [ISO, 2017] and the JIP terminology standard [Ainslie et al., 2018]. Additions made to the terminology during the course of the project reported here are described in an Annex.

2 Summary of Task 1: Characterize sound pressure measurements

The work summarised here is described in greater detail in the Task 2 report [TNO, 2019].

2.1 Data availability

The Svein Vaage dataset was designed to include measurements of acoustical pressure and particle motion produced by the discharge of airguns of a wide variety of makes and types, operated at various deployment depths and chamber pressures. This study is restricted to sound pressure. Not all of the data originally intended to be gathered were successfully acquired. Practical issues such as storm damage meant that some sensors did not provide data over all the source deployments. Other sensors never produced good-quality data because of calibration problems. Despite this, the Svein Vaage dataset comprises a large volume of high-quality data that may be used to characterise marine-seismic airguns as sources of underwater sound.

2.2 Channel recommendations

A manual review of data quality was performed. This led to the identification of combinations of sequences of airgun discharges and recording channels that contained good data. Three out of twenty channels provided good-quality data over the entire dataset. Some other hydrophones provided data over the entire acquisition period, albeit with lower quality for some sequences.

In the 2007 dataset, the Brüel & Kjær (B&K) hydrophones showed excellent data quality while the Reson hydrophones were considered unsuitable for further analysis due to their poor low-frequency response. AGH hydrophones would be considered suitable for use after an adjustment was applied to make them match the B&K hydrophones but this was only so for frequencies up to 1 kHz.

The 2009/2010 survey was only reviewed for the B&K and AGH 7500C hydrophones because other hydrophones were rejected based on the 2007 analysis. Damage due to a storm during the 2009 acquisition and an entanglement of recording equipment with an anchor caused a further reduction in the availability of good-quality data.

It was recommended that further analysis should progress using channel-sequence combinations with data quality assessed to be 'high'. These are shown in green in Table 1. Approximately 40% of the hydrophone data was found to be of sufficient quality to be used in the current analysis. This recommendation was followed and the subsequent analysis does not include any further contribution from the sensors which were adjudged to have provided lower-quality data. This included the 'nearfield' hydrophones that would normally be used in the calculations of source waveforms.

Physical			Physical		Physical		Physical		Physical		Physical		Physical
Channel			Channel		Channel		Channel		Channel		Channel		Channel
Table 1			Table 2		Table 3		Table 4		Table 5		Table 6	ا _د ا	Table 7
2007	Model	Group	2009/10		2009/10	9	2009/10		2009/10	æ	2009/10	CH2 F	2009/10
HydArr01Bd	B&K 8105	VCoA	Seq 1-26		Seq 27-186	Added	Sq 187-204	_	Seq 205-281	S1KH	Seq 282-307	102	Seq 308-315
HydArr02B	B&K 8105	VCoA	ComArr01-BK-d	Σ	ComArr01-BK-d	M20	CornArr01-BK-d	Removed	CornArr01-BK-d	added 51kHz	ComArr01-BK-d	Rem oved 102kHz Fs	CornArr01-BK-d
HydArr03B	B&K 8105	VCoA	ComArr02-BK-n	STORM	ComArr02-BK-n	Tangle.	CornArr02-BK-n	Rem	CornArr02-BK-n		ComArr02-BK-n		ComArr02-BK-n
HydArr04B	B&K 8105	VCoA	ComArr03-BK-n	"	CornArr03-BK-n*	or Ta		M20		Sens		Insort	
HydArr05B	B&K 8105	VCoA	ComArr04-BK-n		CornArr04-BK-n†	Anchor	CornArr04-BK-n			M20 Sensors		M20 Sensors	
HydArr06B	B&K 8105	VCoA	ComArr05-BK-n		ComArr05-BK-n					9		Σ 9	
HydArr07B	B&K 8105	VCoA	ComArr06-BK-n		ComArr06-BK-n		CornArr06-BK-n		CornArr06-BK-n		ComArr06-BK-n		CornArr06-BK-n
HydArr08B	B&K 8105	VCoA	ComArr07-BK-n		ComArr07-BK-n		CornArr07-BK-s						
HydArr09B	B&K 8105	VCoA	ComArr08-BK-n		ComArr08-BK-n		CornArr08-BK-n		CornArr08-BK-n		ComArr08-BK-n		CornArr08-BK-n
HydArr10Bs	B&K 8105	VCoA	ComArr09-BK-n		CornArr09-BK-n‡						ComArr09-BK-n		CornArr09-BK-n
CenArr01d	B&K 8105	VCeA	ComArr10-BK-s		ComArr10-BK-s§								
CenArr02	B&K 8105	VCeA	CentArr01-BK-d		CentArr01-BK-d		CentArr01-BK-d		CentArr01-BK-di		CentArr01-BK-d		CentArr01-BK-d
CenArr03s	B&K 8105	VCeA	CentArr02-BK-d		CentArr02-BK-o#		CentArr02-BK-s		CentArr02-BK-d		CentArr02-BK-d		CentArr02-BK-d
NF01	AGH 7500C	NFC	CentArr03-BK-s										
NF02	AGH 7500C	NFC	NF01		NF01		NF01- P		NF01		NF01- P		NF01- P
NF03	AGH 7500C	NFC	NF02		NF02		NF02 - F		NF02		NF02 - F		NF02 - F
NF04	AGH 7500C	NFC	NF03		NF03		NF03 - D		NF03		NF03 - D		NF03 - D
HydCen00Rd	ResonTC4014	VCeA	NF04		NF04		NF04 - A		NF04		NF04 - A		NF04 - A
NFgun	AGH 7100C	Sroe											
HydArr00Rd	ResonTC4014	VCoA											

Channel 2 had poor repeatability for sequences 7-16. Channel 13 had	Good	* Dead or load seq 150-157, 173-186.				
worse repeatability than channel 12	Fair Fair	† Dead or bad segs				
	Poor	154-161, 181-186.				
		‡ Dead seq 104-186.				
Good		§ Issue seq 111.				
Poor		# Low-frequency distortion during sequences 43-186				
Table 1:						
High-level summary of channel availability and data quality.						

Gun Type	Seq. 1 - 26	Seq. 27 - 186		Seq. 187 - 204		Seq. 205 - 281		Seq. 282 - 307	Seq. 308 - 315
G-gun	250,150,60	2x60,2x100,150,		150				150,60	
		3x250							
Bolt 1900		30,120,200				2x90,2x125,2x145			
Bolt 1500	150	80,150,340				2x150,2x155,			
						2x235,2x290			
G-gun II				250,380					
Bolt AGP						2x300,300,			
						2x175,1x175			
Gl-gun						45/105,45g,105i			
						,45/105,75/75,			
						75g,75i,75/75			
Sleeve									20,40,2x40,2x20
igh-level summary o	h-level summary of gun types. Coloured cells show sequences in which guns of type given in first column were used. Gun volumes given in cubic inches.								

2.3 Pre-processing

To correct the raw pressure traces in the SEG-Y files for artefacts introduced in the recording process, and to recover as nearly as possible the sound pressures generated by the airguns at the time of measurement, two main pre-processing stages were followed.

In the first stage, hydrophone recordings were compensated for the frequency-dependent instrument response of the hydrophones. An inverse filter was also applied to account for the low-frequency distortion caused by the Nexus signal conditioner and the PXI Analogue to Digital Converter (ADC) used in the acquisition process. Finally, a high frequency correction was applied for the B&K hydrophones, taken directly from the manufacturer's datasheet, using an assumption of minimum-phase response.

In the second stage of pre-processing, frequency regimes of the data not useful for airgun-signal characterization were removed using a filter with a low cut of 2 Hz and a high cut that is determined by the alias-free bandwidth of the ADC (i.e., 40% of sampling frequency). The precise values of high-cut frequencies used were "rounded down" to match the decidecade (third-octave) bands commonly used in underwater acoustic signal processing. Details of the filters used can be found in [TNO, 2019] under 'signal conditioning'.

2.4 Bioacoustic metrics

The nature of the impact of underwater sound on marine life is an area of active research and there is still considerable uncertainty associated with its prediction. This leads to the existence of a large number of metrics which are used by various authors in the open literature in an attempt to quantify the impact of sound. The most commonly used metrics derive from the primary use of airgun signals: seismic imaging [Vaage et al, 1983]. They include peak sound pressure, bubble-period and primary-bubble ratio, defined as the ratio of the amplitudes of the first peak and the first bubble-peak. Recent interest in the acoustical impact on marine life has necessitated the development of new metrics.

When considering acoustical impacts on marine life, frequency bands and weightings are important. Some species are more sensitive to high-frequency sound and others to low frequency sound.

An extensive list of metrics was proposed in this project, based on considerations of potential impact on marine life. Many of these metrics are critically affected by the bandwidth of the data and this is not constant throughout the Svein Vaage dataset because of the use of different sampling frequencies during different acquisition periods.

To facilitate comparison and to help assess the consequences of the absence of high-frequency signal components from subsets of the data, it was recommended that two sets of metrics be calculated for those parts of the dataset which are sampled at the higher frequency. The first of these used a high-cut frequency matching 40% of the sampling frequency, rounded down to match the upper limits

of the nearest decidecade band. The second matched the lower sampling frequency that was used for a subset of the dataset. This approach provided a set of metrics with a common frequency band across the entire dataset. The metrics with the higher high-cut frequency allowed an assessment to be made of which descriptors of the airguns' acoustic output were affected by signal components beyond the high-cut of the subset of the data in which the lower sampling frequency was used.

2.5 Results

The processing carried out incorporated a large number of combinations of

- · airgun type,
- airgun volume,
- chamber pressure,
- source depth,
- metric.

Example plots showing trends in metrics (such as peak sound pressure) with source-describing parameters (such as chamber pressure) were produced and comparisons made with other examples from the literature.

3 Summary of Task 2: Characterize sources

The work summarised here is described in greater detail in the Task 2 report [TNO, 2020a].

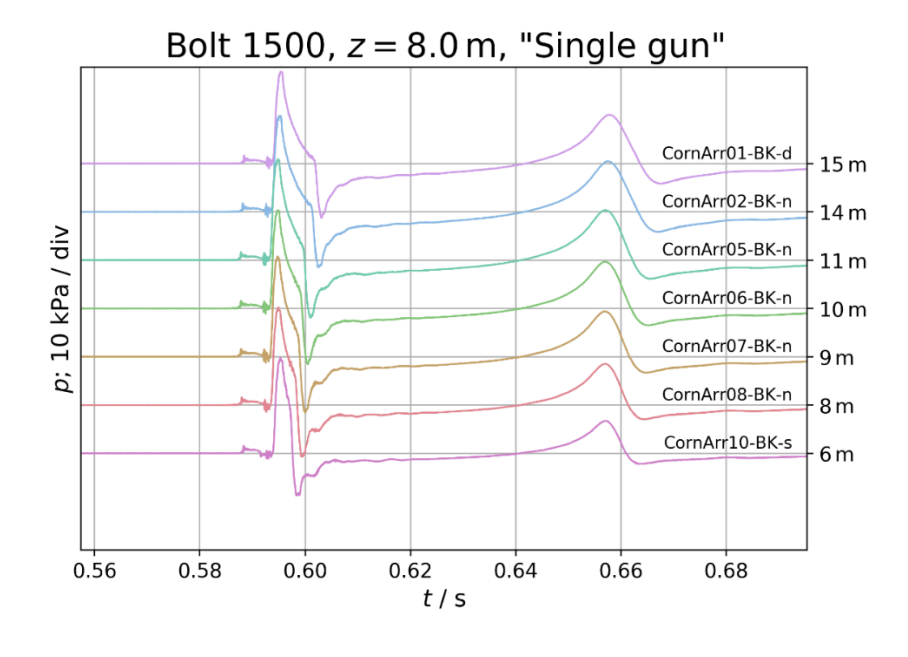
The purpose of the second task was to characterize the airguns by converting sound pressure time series to source waveforms (also known as "notional source signatures"). The source waveform represents the emitted acoustical signal from the source itself; it does not include the effect of the sea surface reflection. The term "source signature" is widely used to mean either the surface affected output or the source waveform. Because of this ambiguity in the meaning of "source signature", the term "source waveform" was preferred.

The source waveform has units of pressure-distance (pascal-metres). However, the source waveform is **not** the pressure measured at 1 m from the source. The form 'pascals at 1 m' is not preferred for use because it is dimensionally wrong and the actual pressure at 1 m from the source is likely to be different from this value because it is in the acoustic near field.

Analysis was restricted to hydrophones with consistently reliable calibrations, which were the Brüel and Kjær hydrophones from the centre and corner arrays. Use of these relatively distant hydrophones was associated with uncertainty in travel-time estimation. This sometimes resulted in a "saw tooth" pattern in the source waveform that was mitigated by carrying out a grid search for the optimal arrival time for the surface-reflected arrival and by averaging the source waveform coherently over channels.

The quality of the resulting source waveforms was quantified by calculating the signal-to-processing-noise ratio (SPNR) for each sequence. The higher the SPNR, the greater the confidence in the inverted source waveform.

Figure 2 shows an example series of measured pressures in the upper panel and the lower panel shows the source waveforms derived from them. This illustrates how propagation from source to receiver is different from a 'one over range' relationship that would make the measured pressure a simple scaled version of the source waveform. Interference between direct and surface-reflected propagation paths causes cancelation and enhancement of acoustic pressure, making the pattern of peaks and troughs in the received pressure very different from those observed in the source waveform.



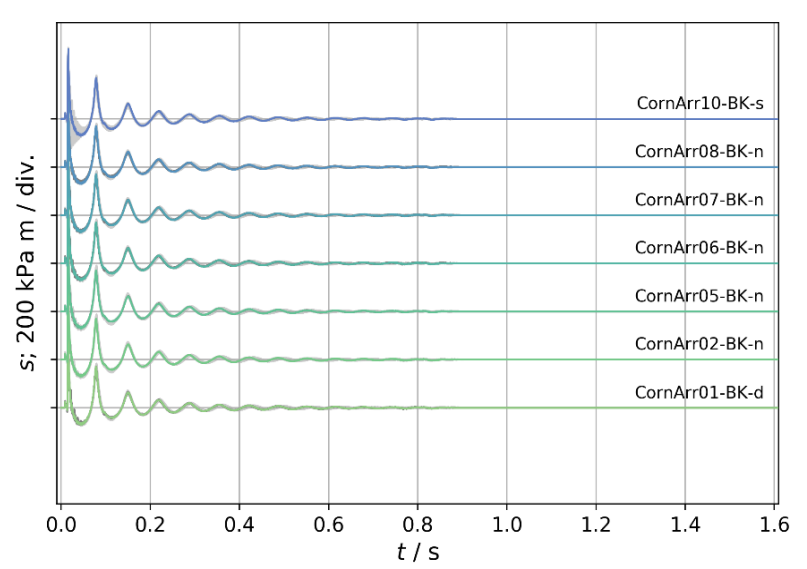


Figure 2 Upper: Waterfall plot of sound pressure (with 10 kPa divisions) versus time (s) recorded for the sixth shot of sequence "seq100_0080L__080_1900_000_C0" (Bolt 1500, 80 in³ = 1.31 L, 8 m depth, 1900 lbf/in² = 13.10 MPa). Text alongside traces gives identifier for measurement hydrophone.

Lower: source waveforms derived from the pressures in the panel above and stacked per sensor. Consecutive shots are plotted in dark grey (barely visible due to good

times of top trace). Note the difference in time axis between the frames.

repeatability). Rejected outliers are shown in light grey in the background (see earliest

The highest peak in the source waveforms shown in Figure 2 is caused by the initial release of air from the airgun. The air released by the airgun forms a bubble which expands until external hydrostatic pressure causes it to halt and then compresses it. Inward acceleration of the bubble wall causes it to collapse and rebound and the process then repeats over a number of cycles. The peaks in the source waveform that follow the highest peak are caused by rapid radial expansions of the air bubbles immediately after collapse. Details of the shape of source waveforms may be modified by careful design of airguns' physical structure, e.g. the shape of their air-outlet ports [Coste et al, 2014].

gun type	G-gun
volume (in³)	250
volume (dm³)	4.097
depth (m)	2.0
chamber pressure (lbf.in-2)	500
chamber pressure (MPa)	3.447

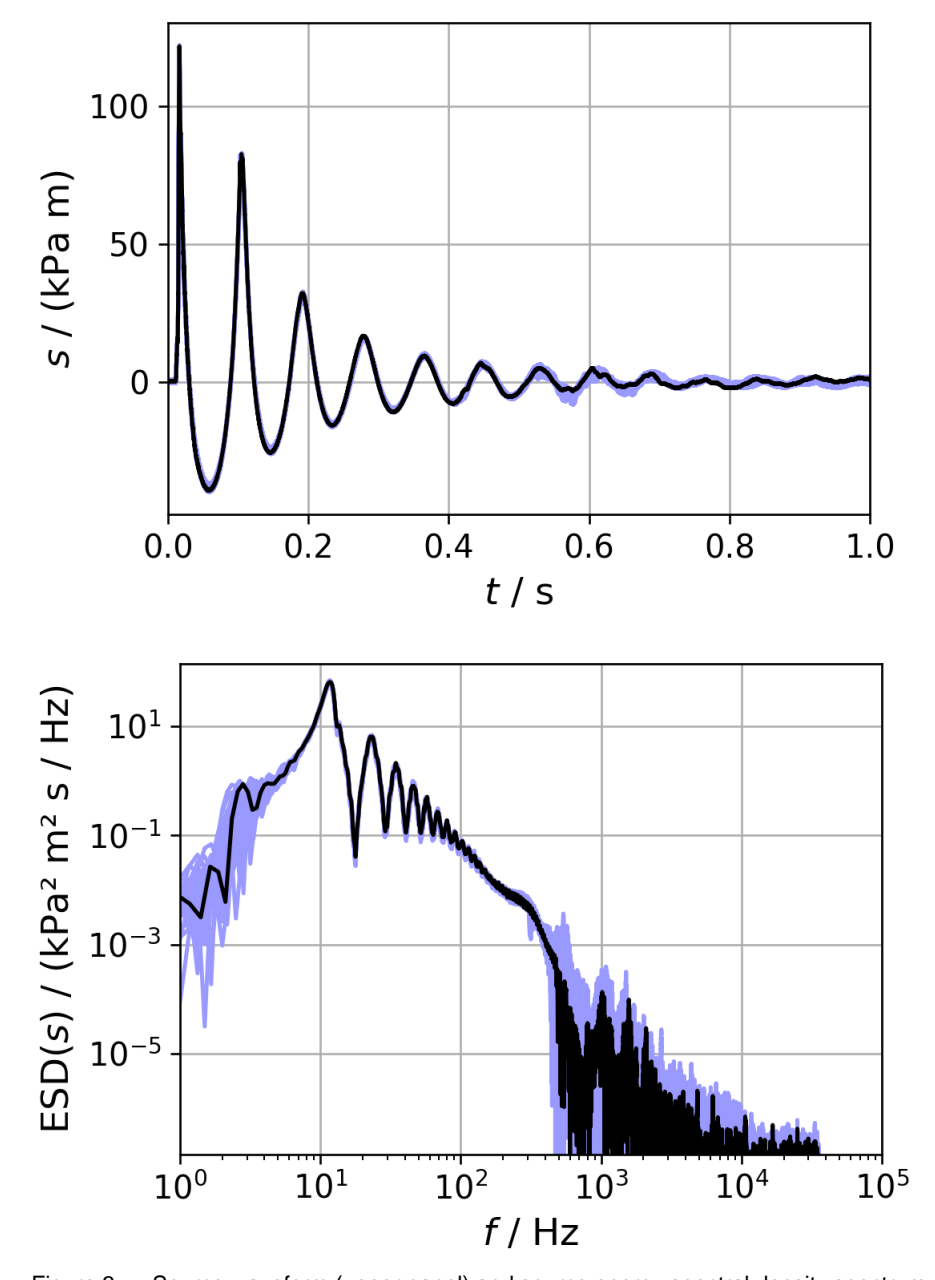


Figure 3 Source waveform (upper panel) and source energy spectral density spectrum (lower panel) for G-gun with properties listed at the top of the figure. Black lines show the representative waveform and spectrum for the sequence, coloured lines show repeatability across the sequence (i.e. multiple discharges with the same nominal settings).

Figure 3 shows the source waveform and energy spectral density spectrum for one sequence of data with properties listed at the top of the figure. The black lines show the representative waveform and spectrum. Coloured lines show repeatability

across the sequence, i.e. the results of multiple discharges with the same nominal settings.

The source waveform plot illustrates the highly repeatable nature of most sequences. The spread across repeated firings only becomes apparent after approximately 0.5 seconds when pressure amplitudes have decreased to approximately one tenth of the peak value observed. At this period and beyond, sound radiation occurs because of repeated collapse and re-expansion of the air bubble formed by the discharge.

The source spectrum plot shows a much wider spread across the sequence. This is perhaps surprising because the spectra are formed by Fourier transforms of the (apparently repeatable) waveforms. The coloured lines are visible at frequencies approximately below 10 Hz and above 300 Hz. For frequencies below 10 Hz, the spread of results is probably caused by external noise sources or by pressure variations at the hydrophone caused by sea-surface waves or vertical motion of the barge from which the hydrophones and aiguns were suspended. For the higher frequencies, sound radiation processes become stochastic, resulting in variation across shots within the same sequence. For the frequencies at which most sound is emitted, repeatability across the sequence is good and the coloured lines cannot be seen beneath the single, representative spectrum.

Plots similar to Figure 3 are shown for all sequences in the Svein Vaage dataset in Annex C to this report [TNO, 2021]

A number of metrics were computed from the source waveform to characterise its properties in the time and frequency domains. These metrics were computed for the mean source waveform for each shot and the statistics (the median, mean and standard deviation of the logarithm of each metric) were computed over shots to quantify shot to shot variation.

To illustrate the physically important relationships between airgun characteristics and acoustical output, regression fits were made between airgun chamber pressure (P), airgun volume (V) and deployment depth (D) and two commonly used metrics. The chosen metrics were the peak squared-signature and the time-integrated squared-signature for the source. These two metrics, when multiplied by a propagation factor (equal to $1/r^2$ in far-field conditions), give peak-squared-pressure and sound exposure at distance r, respectively. The expressions for the source derived were, in decibel terms,

$$L_{S,pk} \approx 211.4 \text{ dB} + 15.2 \log_{10} \frac{P}{1 \text{ MPa}} \text{ dB} + 6.5 \log_{10} \frac{V}{1 \text{ L}} \text{ dB}$$
 (1)
- $0.6 \log_{10} \frac{D}{1 \text{ m}} \text{ dB}$

$$L_{S,E} \approx 195.7 \text{ dB} + 11.3 \log_{10} \frac{P}{1 \text{ MPa}} \text{ dB} + 8.9 \log_{10} \frac{V}{1 \text{ L}} \text{ dB} - 2.3 \log_{10} \frac{D}{1 \text{ m}} \text{ dB}$$
 (2)

Where $L_{S,pk}$ is the zero-to-peak source level in dB re (μ Pa m)² and $L_{S,E}$ is the energy source level in dB re (μ Pa m)²s [ISO, 2017].

The correlation between these regression fits and the data on which they are based is shown in Figure 4.

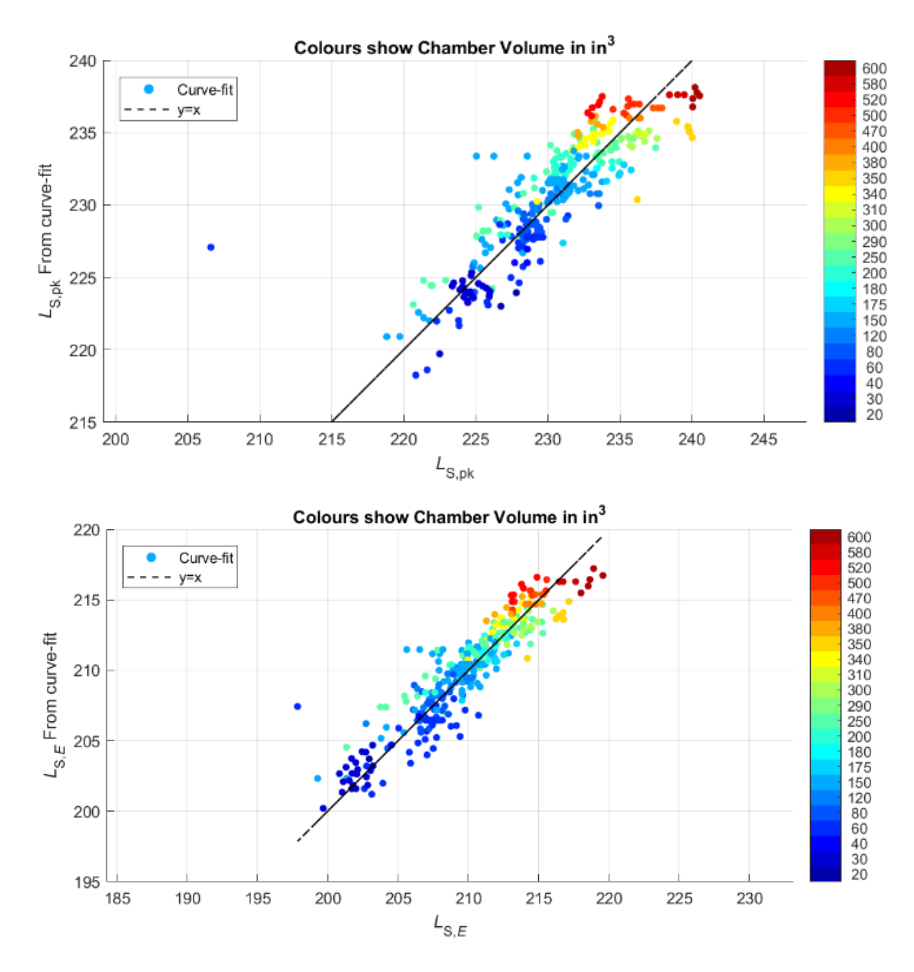


Figure 4 Regression-based metrics plotted as a function of measured metrics: peak source signature level on top, energy source level below. Black line shows the y=x line on which all points would lie in the case of a perfect regression. Marker colour is determined by the volume of the chamber.

The good correlation shown in Figure 4 is illustrative that the source waveforms derived were accurate descriptors of source acoustical output. The rms difference between regression-based and measured metrics was 2 dB in both cases. Comparison between the regression-fit parameters and those reported in the literature [Vaage et al, 1983] showed the expected relationships between peak signatures, chamber pressure, airgun volume and deployment depth.

4 Summary of Task 3: Predict sound field / far-field source signature

The work summarised here is described in greater detail in the Task3 report [TNO, 2020b].

The acoustical output of marine-seismic airguns, measured during the acquisition of the Svein Vaage dataset, was characterised in Task 2 in terms of the 'source waveform', also referred to as the 'notional signature'. This waveform was used to produce the 'surface-affected source waveform', also referred to as the 'far-field signature'. This is defined in such a way [ISO, 2017] that if it is divided by the distance from the sea-surface above the source to a deep hydrophone placed directly below the source, the result is equal to the pressure received on that hydrophone.

In Task 3, the pressure predicted in this way was compared with the pressure measured on the far-field hydrophones in the Svein Vaage dataset. A second prediction of pressure was also made, based on the source waveform and including propagation via direct and surface-reflected paths. The validity of the two 'source characterisations' was investigated in terms of the agreement between predicted and measured sound pressure at deep hydrophones. Agreement was quantified in terms of metrics that describe properties such as sound exposure level, peak sound pressure, rms sound pressure, signal duration, centre frequency, signal bandwidth and bubble period.

In general terms, the comparison of metrics based on predicted and measured sound-pressure at the deep hydrophones indicated that the source characterisations are valid descriptors of the airguns' acoustic output.

Sound exposure levels were shown to be well predicted for frequency bands which contained most of the airguns' acoustical output. Root-mean-square (RMS) mismatch between measured and modelled data was generally less than 3 dB. This is true for broadband data, for most frequency sub-bands and for most frequency-weighted sound exposure levels. Some high frequency bands showed sound exposure levels measured at the deep hydrophones that were significantly affected by background noise, due to the short duration over which airguns emit high-frequency sound and the relative longer duration for the broadband signal. The periods in which airguns release high-frequency sound are those associated with the initial release of air and just after the bubble collapses. Figure 5 shows these periods in pressure signals recorded for a set of sequences. The spectrograms in the right-hand column of the figure show vertical lines indicating significant energy at high frequencies at times corresponding to the peaks in the source waveforms shown in the left-hand column.

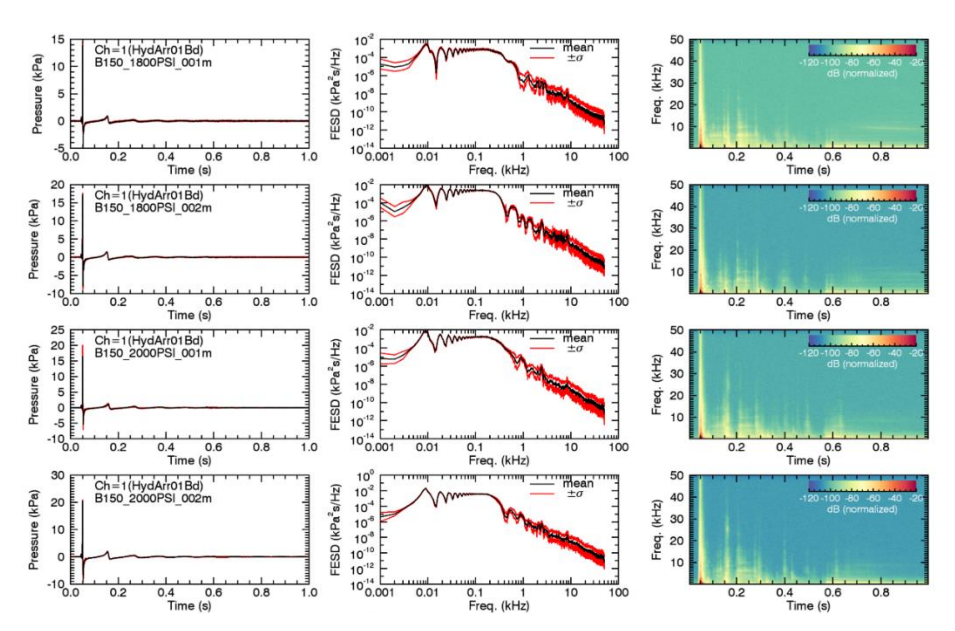


Figure 5 (Reproduced from [TNO, 2019]). Example of a sequence summary plot showing mean sound pressure traces (left), spectra (middle), spectrogram (right) on channel 1 (corner hydrophone array) for the first four sequences recorded during 2007.

A similar effect was observed for frequency-weighted metrics of sound exposure that emphasised high-frequency components of signals.

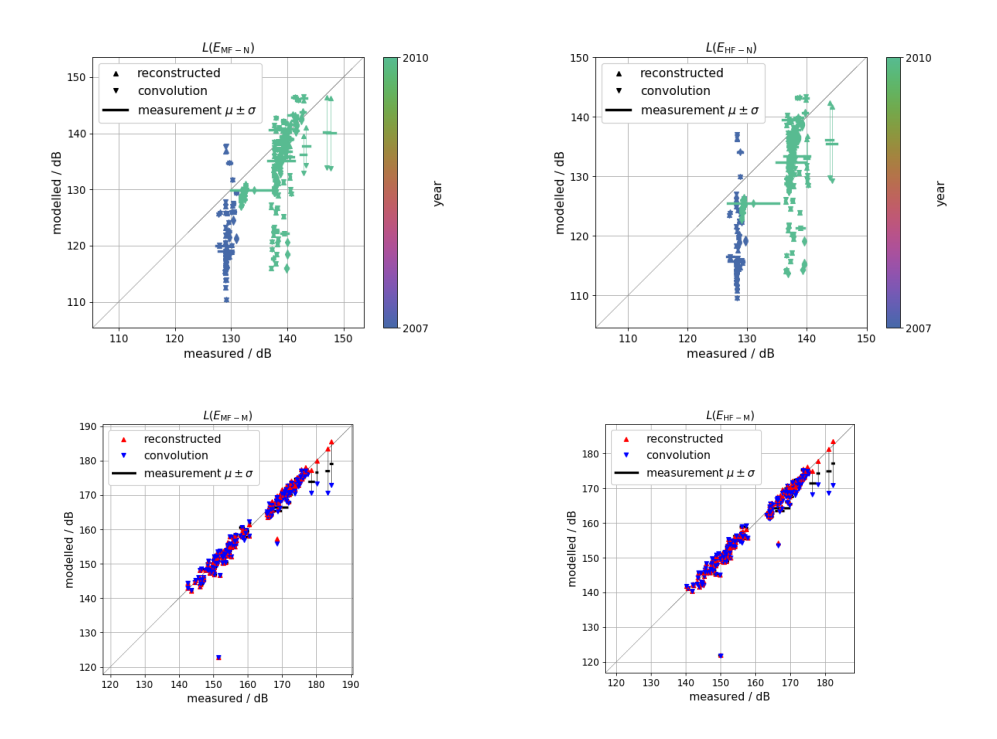


Figure 6 Model-measured comparison of sound exposure level using frequency weightings for medium-frequency cetaceans (left column) and high-frequency cetaceans (right column). Upper panels show results for NMFS weighting [NMFS, 2018] with markers colour-coded by measurement year. Lower panels show results calculated using M-weightings [Southall et al., 2007].

This phenomenon is illustrated in Figure 6 which shows scatter plots of metrics of sound exposure level, weighted for medium frequency and high-frequency

cetaceans. Markers in the figure are plotted at x-coordinates determined by metric values calculated from measured pressures and y-coordinates calculated from predicted pressures based on the source waveform (denoted 'convolution') and surface-affected source waveform (denoted 'reconstructed'). The upper panels show metrics calculated using NMFS weighting [NMFS, 2018] with markers colourcoded by measurement year. Lower panels show results calculated using Mweightings [Southall et al., 2007]. The NMFS weighting places greater emphasis on higher frequencies (>8 kHz) and this is shown to result in poor correlation between metrics based on measured and predicted pressures. This in turn arises from the calculation of sound exposure level using a time-integration period covering the entire duration of the broadband pulse. High-frequency noise is present throughout this period but high-frequency energy was seen to be present only intermittently mainly during pressure peaks associated with the initial release of air. Integration over the entire duration introduced a substantial amount of acoustical energy from background noise, while not significantly adding to signal energy at times outside the initial peak. It is this effect which caused the measured metrics to concentrate into two groups strongly correlated with measurement year, the grouping being likely to be a result of different ambient noise conditions across the two-year period of the Svein Vaage measurements. The lower panels show similar plots for the Mweightings and their increased SNR at lower frequencies results in good correlation between metrics based on measured and predicted pressures.

The source characterisations were also validated in terms of their ability to predict peak and root-mean-square sound pressures to within an RMS mismatch of 2 dB and a bias that was negligible in comparison.

Agreement between measured and predicted duration, central frequency and bandwidth, was observed to vary with the detailed definitions of the various metrics intended to quantify these properties. This was taken to indicate strengths and weaknesses of the various metric definitions and was not related to the validity of the source characterisations.

Bubble period was shown to be well predicted except for a small subset of cases where data showed poor repeatability over sequences of measurements.

5 Data format of Numerical Project Outputs

The project reported here produced a large amount of output data describing:

- Measured sound pressures after the application of pre-processing.
- Source waveforms (also referred to as notional source signatures) for all tested airguns.
- Surface-affected source waveforms (also referred to as far-field source signatures) for all tested airguns.
- Metrics describing source waveforms and measured sound pressures.

All data are stored in the open standard hdf5. This data format allows easy reading in various data analysis tools, such as e.g. Matlab, Python, etc. We choose to write the dataset only using the dataframe function 'to_hdf' from the Pandas library, to guarantee uniformity of the dataset and consistency in the format. Users of the dataset who are free to choose their tooling will have the smoothest experience using Pandas as well. Data are saved in SI base units, unless otherwise indicated.

The data are stored in two-dimensional tabular data structures, called 'dataframes', so that they can be exported to e.g. Excel, Matlab tables and various database formats with minimal effort. A reader class is provided for Matlab users which can retrieve the tables, with a very small number of exceptions. These exceptions are tables containing textual data (nomenclature and metadata), and the decidecade spectra of the reconstructed signals. These exceptional tables have been exported to excel for users who may not be able to install python due to restrictions by their systems administrators, or who prefer another program. There is also a small python script provided which can export any dataframe to an excel spreadsheet.

The formats of the data files are discussed and illustrative examples are given in Annex B. Supporting information regarding relevant open-source software can be found in the following locations:

- https://pandas.pydata.org/pandas-docs/stable/reference/io.html#hdfstorepytables-hdf5
- https://pandas.pydata.org/pandasdocs/stable/reference/api/pandas.DataFrame.to_hdf.html#pandas.DataFrame.t o hdf

6 Discussion and Recommendations

The Svein Vaage dataset represents a valuable resource for the characterisation of the acoustical outputs of marine-seismic airguns.

The quality of recorded data varied across measurement sensors and the analysis carried out in this project was restricted to only those data of the highest quality. There remains the possibility that even more value could be extracted from the dataset if effort were to be expended in overcoming the difficulties in calibration associated with some sensors. In particular, the work reported here did not attempt to investigate the data recorded by particle-motion sensors deployed during the measurement campaign, nor did it consider the poorly calibrated data from the Reson hydrophones placed close to the source.

The hypothesis that the source waveforms developed in this project represent good descriptions of airguns' acoustical output was supported by the observation of good correlation between metrics describing those characterisations and the basic physical properties of the airguns: chamber pressure, airgun volume and deployment depth. The validity was further supported by similarities between those relationships and similar expressions from the literature. Good agreement between sound pressures measured at far-field hydrophones and pressures predicted from the source waveforms also supported the hypothesis.

The poorest agreement between sound pressures predicted using the source waveforms and measured on far-field hydrophones was observed for metrics that placed emphasis on the highest (approximately more than 8000 Hz) frequencies. At these frequencies, airguns' acoustical emissions represent a very small part of their total output and energy transmission is concentrated into periods very much less than the duration of the total (broadband) signal. This means that integrated energy output calculated over the total duration is significantly affected by background noise that is present for the entire duration of the signal.

These considerations notwithstanding, the source waveforms derived from the Svein Vaage measurements represent an important and highly useful dataset for use in studies concerned with predicting the acoustical output of marine-seismic airguns.

7 Conclusions

Measurements of sound pressure recorded at hydrophones in the vicinity of marineseismic airguns were used to characterise their acoustical output. The validity of the source characterisations was demonstrated via regressions based on metrics describing the acoustical output in terms of peak values and time-integrated squared-signature. These fits were shown to agree with similar fits from the open literature and to predict metrics to within ~ 2 dB.

The validity of source characterisations was further demonstrated by comparison of measured sound pressure at far-field hydrophones and predictions of sound pressure made using the source characterisations.

The validity of source characterisations at the highest frequencies considered (> 8 kHz) remains subject to considerable uncertainty because airguns transmit energy at these frequencies for only a small proportion of their signals' total duration. Consequently, metrics such as energy source level that are integrated over the entire duration of the pulse are affected significantly by background noise. The measures required to solve this problem are complex and worthy of further study.

There is the possibility that further value could be extracted from the dataset of measured data if remaining problems with calibration of some sensors could be solved.

Despite this, the source waveforms derived from the Svein Vaage measurements are very valuable for predicting the acoustical output of marine-seismic airguns.

8 References

- [Ainslie et al., 2016]]Ainslie, M. A., Halvorsen, M. B., Dekeling, R. P., Laws, R. M., Duncan, A. J., Frankel, A. S. & Sertlek, H. Ö. (2016, July). Verification of airgun sound field models for environmental impact assessment. In Proceedings of Meetings on Acoustics 4ENAL (Vol. 27, No. 1, p. 070018). ASA.
- [Ainslie et al., 2018] Michael A. Ainslie, Christ A.F. de Jong, Michele B. Halvorsen, Darlene R. Ketten. UNDERWATER ACOUSTICS - TASK 1: TERMINOLOGY. A report prepared by TNO for the Joint Industry Programme on E&P Sound and Marine Life. JIP Topic - Sound source characterisation and propagation. March 2018.
- [Coste et al, 2014] Coste, E., Gerez, D., Groenaas, H., Larsen, O. P., Wolfstirn, M., Hopperstad, J.-F., . . . Padula, M. (2014). Attenuated high-frequency emission from a new design of air-gun. In SEG Technical Program Expanded Abstracts 2014 (pp. 132-137). Society of Exploration Geophysicists.
- [ISO, 2017] ISO 18405 Underwater acoustics Terminology (Organization for International Standardization, Geneva, 2017).
- [Southall et al., 2007] B. L. Southall, A. E. Bowles, W. T. Ellison, J. J. Finneran,
 R. L. Gentry, C. R. Greene Jr., D.Kastak, D.R. Ketten, J. H. Miller, P.
 E. Nachtigall, W. J. Richardson, J. A. Thomas & P. L. Tyack. (2007). Aquatic Mammals, 33(4), 411.
- [NMFS, 2018] National Marine Fisheries Service (NMFS). 2018 Revision to: Technical Guidance for Assessing the Effects of Anthropogenic Sound on Marine Mammal Hearing (Version 2.0): Underwater Acoustic Thresholds for Onset of Permanent and Temporary Threshold Shifts. U.S. Dept. of Commerce., NOAA. NOAA Technical Memorandum NMFS-OPR-59, 167 p. (2018)
- [TNO, 2016] TNO Quotation number: 919471 "Airgun signature and sound field characterisation using Svein Vaage single airgun and airgun cluster measurements". December 2016.
- [TNO, 2019] TNO Report number: TNO 2018 R11079 "Report on Task 1B of project "SVOW OGP JIP airgun measurements": Characterising Sound Pressure measurements". March 2019.
- [TNO, 2020a] TNO Report number: TNO 2019 R11019 "Report on Task 2 of project "SVOW OGP JIP airgun measurements": Characterise sources". February 2020.
- [TNO, 2020b] TNO Report number: TNO 2020 R10875 "Report on Task 3B of project "SVOW OGP JIP airgun measurements": Compare Pressures". December 2020.
- [TNO, 2021] TNO Report number: TNO 2020 R11609 "Report on Task 4 of project "SVOW OGP JIP airgun measurements": Reporting Annex C: Comprehensive overview of source waveforms and spectra. May 2021.
- [Vaage et al. 1983] Vaage, S., K. Haugland, and T. Utheim. "Signatures from single airguns." Geophysical Prospecting 31, no. 1 (1983): 87-97.

9 Signature

The Hague, May 2021

Drs. C.M. Ort

Research manager

TNO

Acoustics & Sonar

Mark Prior

Author

A Additions to Underwater Acoustics Terminology Arising from the Study

Acoustical terminology follows ISO 18405:2017 and the JIP terminology standard (Ainslie et al., 2018). Additional terms and definitions are listed in Table A.1. In addition, the reader is referred to [TNO, 2019] for terminology specific to source metrics.

Table A.1 Glossary of terms used in this report.

Term	Definition
airgun volume	volume of the space in which the compressed air of an airgun is constrained before it is released into the surrounding water NOTE: for a GI gun this is the sum of the volumes of the generator and injector chambers
chamber pressure	difference between pressure of the compressed air inside the airgun just before it is fired and atmospheric pressure
primary peak	high pressure peak caused by the initial release of the air bubble and corresponding to the first arrival
rms	root-mean-square
secondary peak	high pressure peak corresponding to the first collapse of the air bubble NOTES: The secondary peak is sometimes referred to as the "first bubble peak". The secondary peak can be higher than the primary peak.
sequence	all traces collected in a single SEG-Y file
	NOTE: This corresponds to a collection of repeated shots of a single gun (or cluster), on a single day, deployed at a specific depth at a specific firing pressure. Sequences also typically contain pre- and post-shot background noise recordings.
shot	single firing of an airgun or airgun cluster during a sequence
	NOTE: Shots are numbered in order that they are recorded in the SEG-Y files (background noise recordings are also counted in the shot indexing, for simplicity).
source waveform synonym: notional source signature	product of distance in a specified direction, r, from the acoustic centre of a sound source and the delayed far-field sound pressure, p(t – t0 + r/c), for a specified time origin, t0, if placed in a hypothetical infinite uniform lossless medium of the same density and sound speed, c, as the actual medium at the location of the source, with identical motion of all acoustically active surfaces as the actual source in the actual medium
	NOTE 1: From ISO 18405 (so far verbatim) NOTE 2: The source waveform represents the emitted acoustic signal from the source itself; it does not include the effect of the sea surface reflection. The term "source signature" is widely used to mean either the surface affected output and the source waveform. Because of this ambiguity in the meaning of "source signature", the term "source waveform" is preferred.
trace	single, contiguous time-series record (e.g., pressure versus time) stored in a SEG-Y file, of 4 seconds or 6 seconds duration
wind speed	average wind speed at specified height and location, averaged over specified duration

B Data format of numerical project output

B1. Overview of dataframes per file

The following gives an overview of the files comprising the dataset and the dataframes they contain. Files and dataframe names are typeset in monospace ('typewriter') font, where file names are recognizable by the extension .hdf5 and the paths to the dataframes within these files always start with a slash (/). Variable parts of file names and dataframe names (such as **sequence** or **sensor**) are set in **bold italics**.

metadata.hdf5
/nomenclature

Overview of metrics and some other quantities; the columns are:

- field name
 - Abbreviation of the mathematical symbol used to refer to the metric in datastructures, when used in reference to a (measured or reconstructed) pressure trace
- symbol
 mathematical symbol for the metric in tex code, when used in reference
 to a (measured or reconstructed) pressure trace
- units
 units of the metric, when used in reference to a (measured or reconstructed) pressure trace
- si multiplier multiplier to apply to convert to SI base units (e.g. 1 for seconds, 106 for megapascals)
- field name (source)
 - Abbreviation of the mathematical symbol used to refer to the metric in datastructures, when used in reference to a source trace
- symbol (source)
 mathematical symbol for the metric in tex code, when used in reference
 to a source trace
- units (source)
 - units of the metric, when used in reference to a source trace
- power in dB conversion
 - the variable *n* in the expression $L_x = 10 \log_{10}(x/x_{ref})^n$ dB.
- log10 of dB reference log10 of x_{ref} expressed in SI base units
- description
 - short description of the metric, when used in reference to a (measured or reconstructed) trace
- description (source)
 short description of the metric, when used in reference to a source trace

/sequences

Overview of the sequences with associated metadata; the columns are:

 file_name identifier string used to uniquely refer to a sequence

- year
 - 2007 or 2010
- gun type
- volume (in^3)

airgun volume in US customary system

- volume (dm³) airgun volume in SI units
- depth (m)
- chamber pressure (lbf.in^-2)
- chamber pressure (MPa)
- separation (cm)
- description
- sample rate (Hz)

/soundspeed profiles/sequence

Measured sound speed as function of depth

/sensor positions/sequence

Sensor position (x, y, z) in meters. z is up, consistent with the original dataset, so depth is -z. Sign of x and y may vary but was irrelevant for the current processing. Columns are sensor identifiers

```
reconstructions.hdf5
```

/ddec **sampling frequency** Hz

Decidecade spectra in Pa s / Hz; columns are centre frequencies in Hz, rows are sequences

/metadata

- file name
 - sequence identifier
- shot nr

shot number of the source waveform used for the reconstruction

- sensor id
 - id of the sensor for which the trace is reconstructed
- sensor x (m)
- sensor y (m)
- sensor z (m)

coordinates of the sensor

sample rate (Hz)

sample rate of the trace

/metrics

- Values of the metrics computed for the reconstructions, per sequence /traces (Pa) sampling_frequency Hz
- Reconstructed pressure traces, per sequence

```
reconstruction__spectra.hdf5
/spectra (Pa^2 s Hz^-1) sampling_frequency Hz
```

 Exposure spectral density spectra of the reconstructed pressure traces, per sequence

```
sources__metadata.hdf5
/metadata
```

Columns: sample rate (Hz), shot nr and soundspeed per sequence /metrics

/masks/**sequence**

```
extraction. These masks indicate which pressure traces were used.
    The index 'all' refers to shot numbers for which all sensors were discarded
sources spectra sampling_frequency Hz.hdf5
   /spectra (Pa<sup>2</sup> m<sup>2</sup> s Hz<sup>-1</sup>) sampling frequency Hz
    Source spectrum
sources traces sampling frequency Hz.hdf5
   /traces (Pa) sampling frequency Hz
    Source waveforms; one column per sequence, row are timestamps. Shot
    numbers can be found in sources metadata.hdf.
preprocessed measurements/sequence metrics.hdf5
   /metrics/shots/metric (units)
    Metrics per shot number and sensor
   /ddec/shots (Pa^2 s)/sensor
    Decidecade spectra per sensor
preprocessed measurements/sequence traces sensor.hdf5
   /noise (Pa)
    Traces per shot number
   /shots (Pa)
    Traces per shot number, for recordings without airgun shot
preprocessed measurements/sequence spectra sensor.hdf5
```

Not all shot numbers and sequences were used for the source waveform

Metrics of the source waveforms per sequence

B.2 Examples of data tables contained in the dataset

Source waveforms per shot number

sources/sequence_traces_sensor.hdf5

/shots (Pa^2 s Hz^-1)

Spectra per shot number

/traces (Pa m)

This section contains a section of an example table containing a sequence of shot traces and a section of an example table of a metric.

Example of a dataframe containing pressure traces

```
hdf5 file: ./preprocessed_measurements/B150_1800PSI_001m__traces__HydArr01Bd.hdf5
                                 dataframe: /shots (Pa)
                                                                                                                                                                                                                                                                                                                                                                                                                                                                       8 ... 52 53 54
                                                                                                                                                                                                                                                                                                                                                                                                                                                                                                                                                                                                                                                                                                                                                                                                                                                                                                             55
shot nr
 time (ns)
                                                                                                                                                                                                                                                                                                                                                                                                                                                                                                                         . . .
 00:00:00 13.534032 1.792337 4.588311 0.553060 ... -23.280431 -22.912326 -34.199056 21.066242
00:00:00.00010 16.091645 0.901424 4.169092 5.979970 ... -36.061328 -27.277891 -40.356465 21.788687
   00:00:00.00000 15.108667 1.103449 2.220247 1.888206 ... -29.053612 -23.409237 -29.940488 21.568844
 00:00:00:00.00030 \quad 17.485492 \quad 1.300452 \quad 4.050669 \quad 2.387836 \quad \dots \quad -30.300620 \quad -25.023543 \quad -31.613546 \quad 20.417260 \quad -20.417260 \quad 
 00:00:00.00040 15.733501 -1.779622 5.896622 4.372298 ... -31.865218 -26.375314 -34.538127 22.071657
                                                                                                                                                                                                                                              ...
                                                                                                                                                                                                                                                                                                                                               ...
                                                                                                                                                                                                                                                                                                                                                                                                                                                                                                                                                                                                                                                                              . . .
                                                                                                                                                                                                                                                                                                                                                                                                                                                                           ... ... ...
                                                                                                                                                                                                   . . .
 00:00:05.999960 \qquad 2.901334 \ -0.062384 \quad 1.712869 \ -14.636232 \quad \dots \quad 18.612008 \quad -8.629125 \quad -0.158085 \quad 23.084300 \quad -0.062384 \quad 1.712869 \quad -0.062384 \quad 1.712869 \quad -0.062384 \quad -0.062384
 00:00:05.999970 3.495332 0.627614 1.934842 -14.024511 ... 16.773002 -9.614031 -1.780812 22.992908
 00:00:05.999980 \quad 1.746079 \; -0.311649 \quad 1.315339 \; -16.367006 \quad \dots \quad 24.457082 \quad -7.253454 \quad 4.649355 \quad 23.463504 \quad 1.315339 \quad -16.367006 \quad \dots \quad 24.457082 \quad -7.253454 \quad 4.649355 \quad 23.463504 \quad -1.0167006 \quad -1.01670006 \quad -1.01670006 \quad -1.01670006 \quad -1.01670006 \quad -1.01670006 \quad -1
 00:00:05.999990 \qquad 4.755487 \quad 0.228450 \quad 2.113662 \quad -12.422206 \quad \dots \quad 11.612467 \quad -10.601586 \quad -6.056504 \quad 22.455405 \quad -10.601586 \quad -10
   [600000 rows x 51 columns]
```

Example of dataframe containing values of a metric

```
hdf5 file: ./preprocessed_measurements/B150_1800PSI_001m__metrics.hdf5
   dataframe: /metrics/shots/E tot (Pa^2 s)
         HydArr01Bd HydArr03B HydArr04B ...
                                                      HydArr09B CenArr01d
sensor
                                                                                 CenArr03s
shot nr
      233687.939347 232512.609747 218563.934566 ... 138661.081752 23155.962872 205015.017479
      244921.640259 244736.568876 230190.899090 ... 149738.568595 24336.432288 209401.484970
      241312.956718 241728.095334 226926.531423 ... 146879.649020 24150.609405 207939.535259
       255676.357982 257302.325760 242467.322400 ... 162755.604467 24064.538977 211698.546748
8
      243541.428526 244713.508209 230647.669264 ... 152035.405036 23570.843407 208589.881662
                                   ... ...
51
     177734.852164 174039.369113 159808.904105 ... 98433.702143 23996.097278 214692.526315
52
      165027.885994 159942.975151 145778.684586 ... 87326.334927 23708.284252 208376.188977
      180036.094919 172866.645203 158048.761287 ... 94419.045204 23870.047230 216191.321598
53
54
       181164.305806 176417.778436 161740.468317 ... 97605.894847 24346.165022 219064.527938
55
       178985.432945 174935.208348 158830.142185 ... 95099.452748 24222.348636 214556.046861
[51 rows x 10 columns]
```

B.3 Code listings

This section lists the code for the Matlab helper class as well as the python script which can be used to export the tables from hdf5 to Excel format

hdf tables.m

```
classdef hdf_tables
   properties
       hdf file name
       hdf info
       table_info
   end
   methods
        function obj = hdf_tables(hdf_file_name)
            obj.hdf_file_name = hdf_file_name;
            obj.hdf_info = h5info(hdf_file_name);
            obj.table_info = cell(0, 5);
           obj = obj.add_paths_from_groups(obj.hdf_info);
           obj.table_info = cell2table( ...
                obj.table_info(:, 2:end), ...
                'RowNames', obj.table_info(:, 1), ...
                'VariableNames', { ...
                'columns_name', 'columns_size', 'rows_name', 'rows_size'});
        end
        function tbl = get_table(obj, path)
            row_names = h5read(obj.hdf_file_name, [path, '/axis1']);
           if isnumeric(row_names)
                row_names = cellfun(@num2str, num2cell(row_names), ...
                    'UniformOutput', false);
            end
           var_names = h5read(obj.hdf_file_name, [path, '/axis0']);
            if isnumeric(var_names)
                var names = cellfun(@num2str, num2cell(var names), ...
                    'UniformOutput', false);
            end
            data = h5read(obj.hdf_file_name, [path, '/block0_values']);
            tbl = cell2table(transpose(num2cell(data)), ...
                'RowNames', row_names, 'VariableNames', var_names);
        end
   end
   methods ( Access = private )
        function obj = add_paths_from_groups(obj, group)
```

```
if ~isempty(group.Datasets)
                for dataset = reshape(group.Datasets, 1, [])
                    switch dataset.Name
                        case 'axis0'
                           columns_size = dataset.Dataspace.Size;
                        case 'axis1'
                           rows size = dataset.Dataspace.Size;
                   end
                end
                obj.table info(size(obj.table info, 1) + 1, :) = { ...
                    group.Name, ...
                    h5readatt(obj.hdf_file_name, ...
                    [group.Name, '/axis0'], 'name'), ...
                    columns_size, ...
                    h5readatt(obj.hdf_file_name, ...
                    [group.Name, '/axis1'], 'name'), ...
                    rows_size};
            end
            for sub_group = reshape(group.Groups, 1, [])
                obj = obj.add_paths_from_groups(sub_group);
            end
        end
    end
end
```

export_helper.py

```
import sys
import pandas as pd
import numpy as np

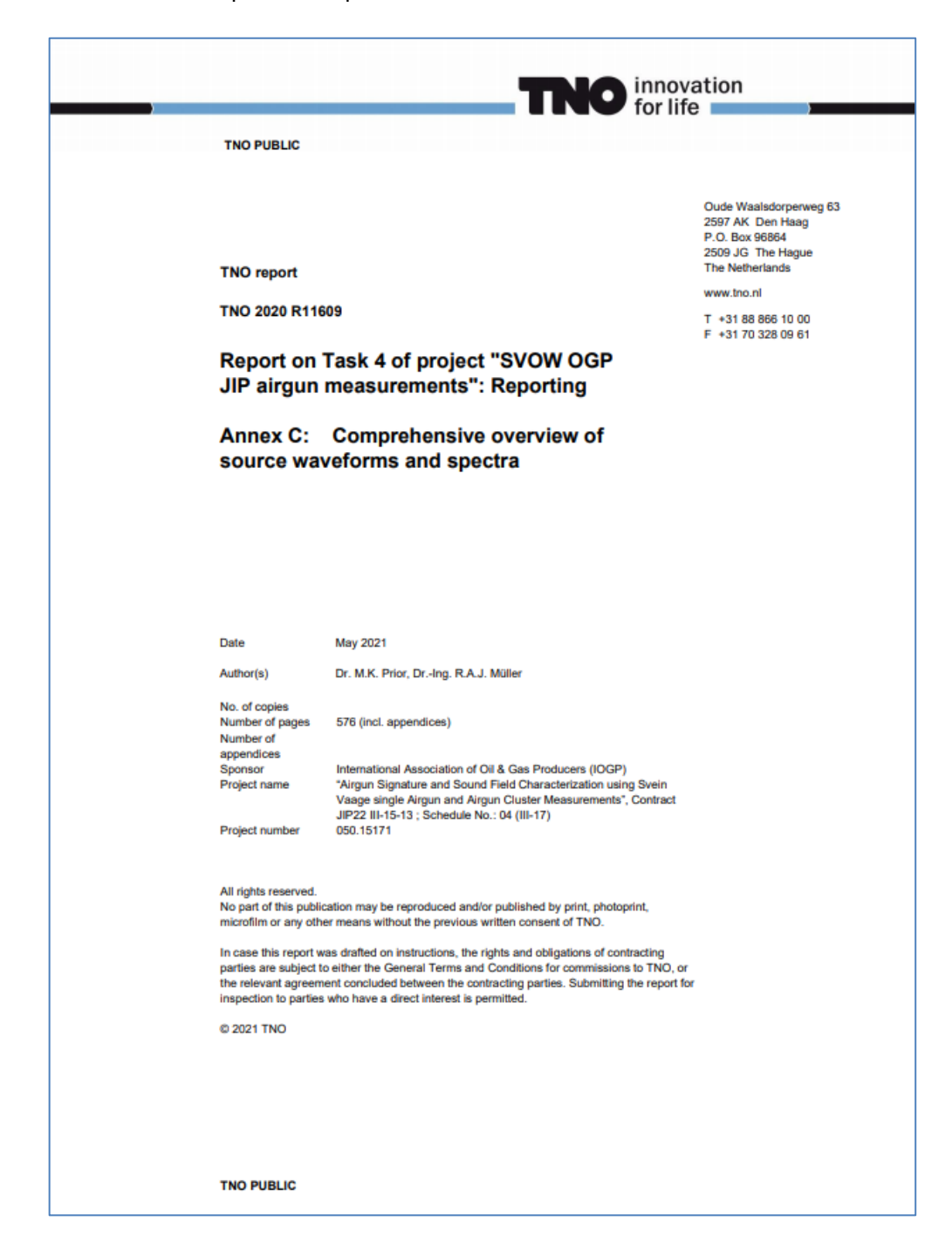
def main(hdf_file=None, dataframe=None, xls_file=None):
    """
    Arguments:
    1: input file (hdf5)
    2: number or path of data set within input file
    3: output file (xlsx)

    Behaviour depends on number of arguments:
    0: print this overview
    1: list dataframes found in hdf5 file
    2: output dataframe as text
    3: export dataframe to excel
    """
    if hdf_file is None:
```

```
print_use_cases()
        return
   with pd.HDFStore(hdf_file, 'r') as h5:
        keys = h5.keys()
        if dataframe is None:
            print_keys(keys)
            return
       try:
            dataframe = keys[int(dataframe)]
        except ValueError:
            pass
        df = pd.read_hdf(h5, dataframe)
   if xls_file is None:
        print(f"""
   hdf5 file: {hdf_file}
   dataframe: {dataframe}
       print(df)
       return
   sheet_name = f'{hdf_file}; {dataframe}'
   if len(sheet_name) > 31:
        sheet_name = sheet_name[-31:]
   df.to_excel(xls_file, sheet_name=sheet_name)
def print_use_cases():
   print()
def print_keys(keys):
   f = f'%{int(np.log10(len(keys))) + 1}d: "%s"'
   for i, k in enumerate(keys):
        print(f % (i, k))
if __name__ == '__main__':
   if len(sys.argv) == 1:
       help(main)
   else:
        main(*sys.argv[1:])
```

C Comprehensive overview of source waveforms and spectra

Annex C of this report is a separate document:



Distribution list Report TNO 2020 R11609

IOGP

Mr. Mike Jenkerson pdf
Mrs. Dianne James pdf
Mrs. Felicite Robertson pdf

JASCO

Mr. Alex MacGillivray pdf Mr. Michael Ainslie pdf

CSA

Mrs. Michele Halvorsen pdf Mrs. Susan Tudor pdf Mr. John Moulton pdf

TNO

Mrs. Iris Hartstra pdf
Mr. Ad van Heijningen pdf
Mr. Christ de Jong pdf
Mr. Roel Müller pdf
Mr. Mark Prior

TNO Bibliotheek locatie Den Haag hard copy &

cd